Letter

Discovery of VU6027459: a first-in-class selective and CNS penetrant mGlu7 PAM tool compound

Carson W Reed, Jacob J Kalbfeisch, Madison J Wong, Jordan P Washecheck, Ashton Hunter, Alice L Rodriguez, Anna L. Blobaum, P. Jeffrey Conn, Colleen M Niswender, and Craig W Lindsley

ACS Med. Chem. Lett., **Just Accepted Manuscript** • DOI: 10.1021/acsmedchemlett.0c00432 • Publication Date (Web): 20 Aug 2020

Discovery of VU6027459: a first-in-class selective and CNS penetrant $mGlu_7$ PAM tool compound

Carson W. Reed,[†,π] Jacob J. Kalbfleisch,[†,π] Madison J. Wong,[†] Jordan P. Washecheck,[†] Ashton Hunter,[‖] Alice L. Rodriguez,[ϕ,‖] Anna L. Blobaum,[ϕ,‖] P. Jeffrey Conn,[ϕ,‖,ψ] Colleen M. Niswender,[ϕ,‖,ψ]* and Craig W. Lindsley[†,ϕ,‖]*

[†]Department of Chemistry, Vanderbilt University, Nashville, TN 37232, United States

[ϕ]Department of Pharmacology, Vanderbilt University School of Medicine, Nashville, TN 37232, United States

[‖]Warren Center for Neuroscience Drug Discovery, Vanderbilt University School of Medicine, Nashville, TN 37232, United States

[ψ]Vanderbilt Kennedy Center, Vanderbilt University, Nashville, TN 37232, USA

[π]*These authors contributed equally*

ABSTRACT: Herein, we report the discovery of the first selective and CNS penetrant $mGlu_7$ PAM (VU6027459) derived from a 'molecular switch' within a selective $mGlu_7$ NAM chemotype. VU6027459 displayed CNS penetration in both mice (K_p = 2.74) and rats (K_p = 4.78), was orally bioavailable in rats (%F = 69.5) and undesired activity at DAT was ablated.

KEYWORDS: metabotropic glutamate receptor, $mGlu_7$, positive allosteric modulator (PAM), VU6027459, Rett syndrome

Holding the distinction of being the most widely expressed metabotropic glutamate receptor in the CNS, $mGlu_7$ is a Group III mGlu receptor (along with $mGlu_{4,6,8}$) that has an extremely low affinity for the endogenous agonist glutamate, and thus, is believed to act as an 'emergency brake' when glutamate levels become elevated.[1,2] There is currently a lack of highly selective and CNS penetrant $mGlu_7$ positive allosteric modulators (PAMs). While an $mGlu_7$ allosteric agonist does exist,[3] its rapid metabolism makes interpretation of in vivo effects difficult to establish.[4] Thus, the therapeutic potential of $mGlu_7$ activation has been ascertained from studies in $mGlu_7$ knock-out mice and with $mGlu_7$ negative allosteric modulators. These studies suggest relevance in treating depression, schizophrenia, cognitive disorders, autism and ADHD.[5-15] Human genetics and *GRM7* polymorphisms have further strengthened these disease associations, while also highlighting the key role of $mGlu_7$ in neurodevelopmental disorders, notably, Rett syndrome.[16-30] Using non-selective Group III PAMs, such as **1**-**4** (**Figure 1**), in combination with $mGlu_7$ NAMs (e.g., **5** and **6**) a pharmacological role for $mGlu_7$ PAMs in Rett syndrome in correcting apneas, as well as social and cognitive dysfunction in mouse models of Rett syndrome, has been discovered.[31-35]

While highly selective and CNS penetrant $mGlu_7$ NAMs, e.g. **6** and related congeners, have been realized, $mGlu_7$-selective PAMs have remained elusive despite multiple high-throughput screening campaigns.[34,36-37] During an $mGlu_7$ NAM optimization campaign surveying ester replacements within an ethyl-8-methoxy-4-(4-phenylpiperazin-1-yl)quinolone carboxylate scaffold exemplified by **7** (VU6009339 $mGlu_7$ IC_{50} = 6.1 μM, >30 μM vs. $mGlu_{1-5,8}$), all moieties surveyed were inactive, save for the cyano group, which engendered a 'molecular switch' to a highly selective (>30 μM vs. $mGlu_{1-5,8}$) and CNS penetrant (rat K_p = 4.7, $K_{p,uu}$ = 0.96) $mGlu_7$ PAM **8** (VU6014181, $mGlu_7$ EC_{50} = 879 nM (pEC_{50} = 6.06±0.18, 51.3±6.6% L-AP_4 max (rat GIRK assay)).[38] Notably, this was the first 'molecular switch' ever encountered with $mGlu_7$ allosteric ligands (**Figure 2**). Based on these exciting data, we also

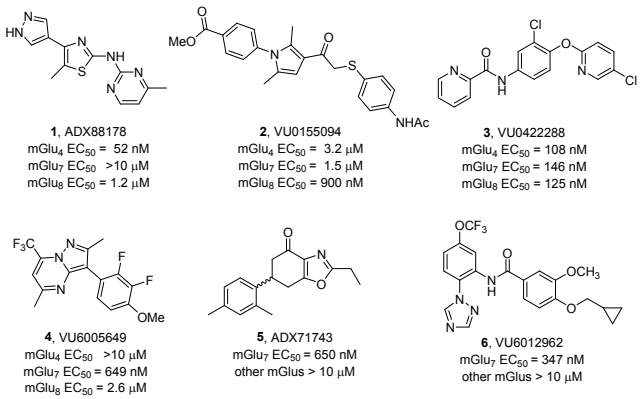

Figure 1. Structures of reported mGlu Group III PAMs **1**-**3**, $mGlu_{7/8}$ PAM **4** and highly selective $mGlu_7$ NAMs **5** and **6**.

evaluated PAM **8** in our rat $mGlu_7$ calcium assay, where similar potency and efficacy were noted ($mGlu_7$ EC_{50} = 1.1 μM (pEC_{50} = 5.98±0.11), 85.1±18.5% L-AP_4 max), further confirming $mGlu_7$ PAM activity. PAM **8** also displayed moderate rat *in vivo* PK (Cl_p = 47.5 mL/min/kg, $t_{1/2}$ = 0.75 hr, V_{ss} = 4.1 L/kg), suitable as a lead for further optimization (rat f_u = 0.032; mouse f_u = 0.051); however, while it was uniformly clean (no inhibition >50%@10 μM) in a Eurofin ancillary radioligand binding panel of 68 different GPCRs, ion channels and transporters, it displayed activity at one 'no go' target – the dopamine transporter (DAT 85%@10 μM, K_i = 430 nM), as global increase in dopamine would mask target validation efforts for $mGlu_7$. Thus, our optimization work-flow would add DAT as a key anti-target to be evaluated and eliminated from a potential *in vivo* probe.

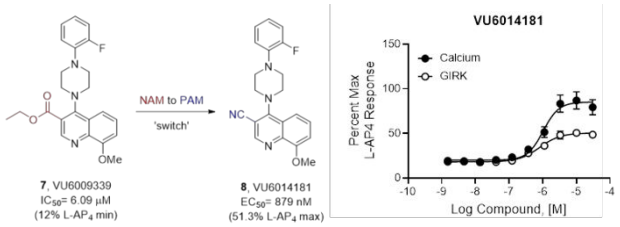

Figure 2. A "Molecular Switch' changes the mode of pharmacology from $mGlu_7$ NAM (**7**) to $mGlu_7$ PAM (**8**). The $mGlu_7$ PAM activity of **8** is comparable in both $mGlu_7$ GIRK (EC_{50}= 880 nM, 51.3% L-AP_4 max) and calcium (EC_{50}= 1.1 μM, 85.1% L-AP_4 max) assays.

In order to optimize **8** for $mGlu_7$ PAM activity, DMPK profile and to ablate DAT activity, we elected to perform a multi-dimensional optimization campaign, surveying a wide range of chemical diversity (**Figure 3**). For the first round of SAR, we elected to hold the 2-fluorophenyl piperazine moiety constant and survey alternatives for the cyanoquinolone core employing the route depicted in Scheme 1. Here, anthranilic

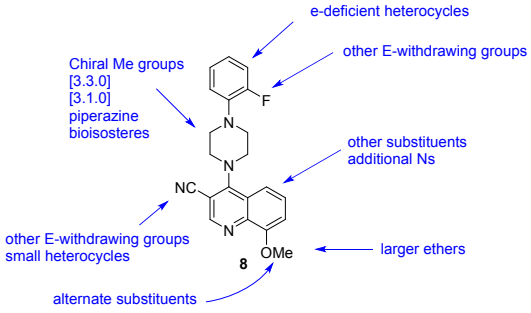

Figure 3. Optimization plan for $mGlu_7$ PAM **8**, surveying broad SAR.

acids **9** are reacted with TMS diazomethane to form methyl esters **10** in 76-90% yield. Treatment of esters **10** with DMF●DMA under microwave irradiation resulted in the formation of amidines **11**, which were carried on crude and reacted with the conjugate base of acetonitrile (formed from the deprotonation of acetonitrile with *n*-BuLi) followed by subsequent treatment with acetic acid to form quinolones **12** in moderate to good yields (58-77%). Quinolones **12** were then heated to 100 °C in neat $POCl_3$ to form chloroquinolines **13** in 78-93% yield. Then, an S_NAr reaction between **13** and 2-fluorophenylpiperazine yielded analogs **14** in good yields (60-82%). Alternatively, a number of 5,6-fused systems **15** were commercially available, and they underwent the S_NAr smoothly to afford analogs **16**.

SAR was steep, with all analogs **16** devoid of $mGlu_7$ PAM activity (see Supporting Information), and only fluorinated con-

Scheme 1. Synthesis of alternate heterocyclic core analogs **14** and **16** of **8**.[a]

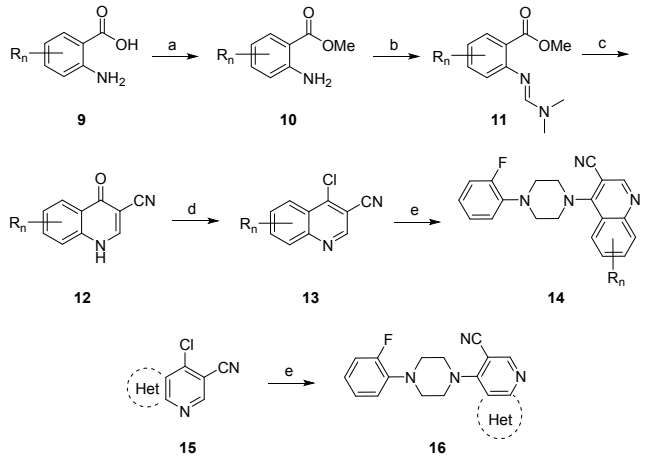

[a]Reagents and conditions: (a) $TMSCHN_2$, PhH:MeOH, 0 °C, 1h, 76-90%; (b) DMF●DMA (Dimethylformamide Dimethylacetal), MeOH, 150 °C (μW), 1 h, 99%; (c) (i) n-BuLi, MeCN, THF, -78 °C,30 min; (ii) AcOH, -78 °C,30 min, 1 hr, 58-77% over two steps; (d) $POCl_3$, 100 °C, 78-93%; (e) 2-Fphenylpiperazine, DMF, 150 °C (μW), 15 min, 60-82%.

geners **14a-d** of **8** (i.e., the 'fluorine walk') displayed $mGlu_7$ PAM activity (**Figure 4**). Of note, **14c** displayed comparable $mGlu_7$ PAM activity (EC_{50} = 1.4 μM, 99% L-AP_4 max) to **8**, but also eliminated DAT activity, indicating that the 6-fluoro moiety was essential to eliminate DAT activity. However, **14c** was moderate to highly cleared *in vitro* (rat CL_{HEP} = 56 ml/min/kg, mouse CL_{HEP} = 87 mL/min/kg), and displayed high protein binding (rat/mouse plasma f_u = 0.010/0.012). In contrast, **14d**, a 6,7-difluro congener, displayed comparable DAT inhibition (K_i = 2.2 μM).

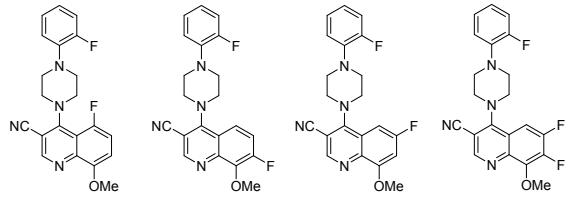

Figure 4. SAR of fluorinated analogs **14** of PAM **8**.

In parallel, we evaluated a wide-range of piperazine bioisoteres, once again maintaining the 2-fluorophenyl moiety, as well as the parent 8-methoxy quinolone core of **8**, or the 6-fluoro core of **14c**. Here, we were surprised to find that only the parent piperazine had $mGlu_7$ PAM activity- all other analogs **17** were inactive (**Figure 5**). Similarly, alternatives to the 2-fluorophenyl moiety in **8**/**14c** proved inactive, further narrowing the scope of the SAR of this PAM series.

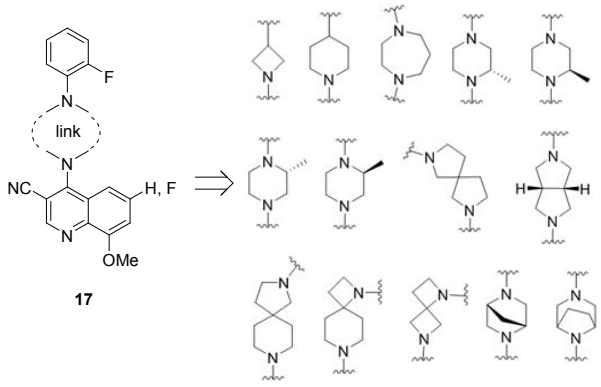

Figure 5. Inactive piperazine bioisosteric analogs **17** of **8**/**14c**.

These data turned our attention to the 8-OMe moiety as a potential site of diversification as well as a potential metabolic soft spot (e.g., oxidative dealkylation). Starting from either **8** or **14c**, demethylation with BBr_3 provided the corresponding phenols **18**/**19** in good yields (**Scheme 2**). A microwave-assisted alkylation reaction afforded the desired ether analogs **20**/**21** in 47-68% yield.

Scheme 2. Synthesis of 8-ether analogs **20** and **21**.[a]

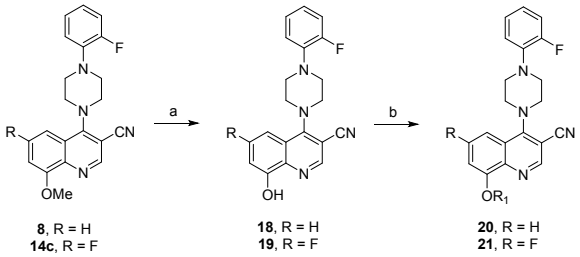

[a]Reagents and conditions: (a) BBr_3, DCM, -78 °C to rt, 16h, 54-76%; (b) R_1Br, K_2CO_3, MeCN, 150 °C (μW), 1 h, 47-68%.

Table 1. Structures and $mGlu_7$ PAM activities of selected analogs **20**/**21**.[a]

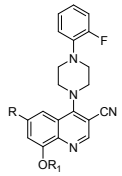

Cmpd No.	R	R_1	$mGlu_7$ EC_{50} (μM)	$mGlu_7$ %L-AP_4 max
18	H	H	>10	90
19	F	H	>10	90
20a	H	CD_3	1.5	73
21a	F	CD_3	1.1	98
20b	H	CF_2H	>10	68
21b	F	CF_2H	3.8	98
20c	H	*i*-Pr	1.25	67
21c	F	*i*-Pr	0.69	88
20d	H		1.8	67
21d	F		>10	23
20e	H		1.3	74
(+)-20e	H		1.1	85
(-)-20e	H		1.1	70
21e	F		0.51	71
20f	H		1.3	88
(+)-20f	H		1.9	77
(-)-20f	H		1.3	89
21f	F		0.65	76

[a] Calcium mobilization assays with rat $mGlu_7/G_{qi5}$-HEK cells performed in the presence of an EC_{20} fixed concentration of L-AP_4; values represent means from one independent experiment performed in triplicate.

Structures and $mGlu_7$ PAM activities of selected analogs **20**/**21** are highlighted in Table 1. The phenolic congeners **18** and **19** were inactive (EC_{50}s > 10 μM), whereas the $–OCD_3$ analogs **20a**/**21a** were equipotent to the parent proteo compounds. PAM activity varies based on the presence or absence of the 6-F moiety, as highlighted in **20b** versus **21b** and **20d** versus **21d**. Sterically bulky and/or lipophilic ethers were generally inactive, save for the iospropoxy derivatives **20c** (EC_{50} = 1.3 μM, 67% L-AP_4 max) and **21c** (EC_{50} = 0.69 μM, 88% L-AP_4 max). Incorporation of Lewis basic sites, as in the case of tetrahydrofuranyl ethers **20e-f**/**21e-f** showed potency comparable to the parent PAMs. However, the racemic **20e** and **21e** were as potent and efficacious as the separated (chiral SFC) single enantiomers (e.g., (rac)-**20e** compared to (+)-**20e**, (-)-**20e** and (rac)-**20f** compared to (+)-**20f**, (-)-**20f**). Overall, very little

texture to the SAR was observed, and the vast majority of analogs evaluated were inactive.

Scheme 3. Synthesis of 8-heterocyclic analogs **23**.[a]

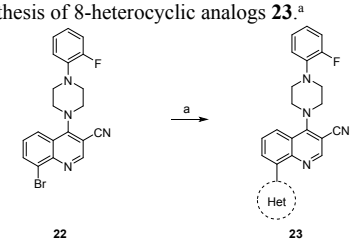

22 **23**

[a]Reagents and conditions: (a) Pd_2dba_3, *rac*-BINAP, NaO*t*Bu, toluene, 110 °C,16h, 32-61%.

Based on the activity of furans **20e**/**21e**, we decided to explore other saturated and aromatic heterocyclic groups in the 8-position via Buchwald-Hartwig chemistry (**Scheme 3**) employing **22** to deliver analogs **23**. As before, SAR was steep, with few active $mGlu_7$ PAMs (**Table 2**). Here, only a single morpholine derivative, **23g**, proved potent (EC_{50} = 1.3 μM, 74% L-AP_4 max), and the importance of the Lewis basic oxygen was pronounced, as the analogous piperidine **23e** was inactive.

Table 2. Structures and $mGlu_7$ PAM activities of selected analogs **23**.[a]

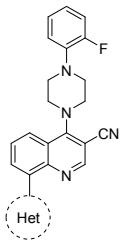

23

Cmpd No.	Het	$mGlu_7$ EC_{50} (μM)	$mGlu_7$ %L-AP_4 max
23a		>10	22
23b		6.7	81
23c		>10	23
23d		>10	22
23e		>10	24
23f		>10	22
23g		1.3	74
23h		7.1	84

[a] Calcium mobilization assays with rat $mGlu_7/G_{qi5}$-HEK cells performed in the presence of an EC_{20} fixed concentration of L-AP_4; values represent means from one independent experiment performed in triplicate.

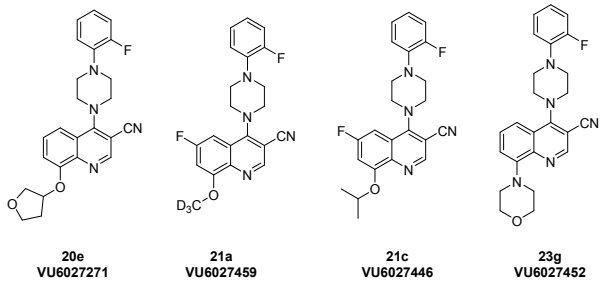

20e VU6027271 **21a** VU6027459 **21c** VU6027446 **23g** VU6027452

Figure 6. $mGlu_7$ PAM tool compound candidates **20e**, **21a**, **21c** and **23g**.

At this point, we elected to perform deeper molecular pharmacology (n = 3 on rat calcium and GIRK HEK lines) and DMPK profiling (**Table 3**) of a selection of $mGlu_7$ PAMs identified thus far (to assess if any had the overall profile to be useful as *in vitro* and/or *in vivo* tool compounds to probe selective $mGlu_7$ activation (**Figure 6**)). All four PAMs showed good CNS penetration in rats, with K_ps >4 and $K_{p,uu}$s >0.79, no DAT activity, and moderate predicted hepatic clearance in rats (comparably high in mouse). All four were highly protein bound in both rat and mouse, as well as in rat/mouse brain homogenate binding. Of these, **21a** (VU6027459) emerged as the most attractive $mGlu_7$ PAM for further profiling with good potency (EC_{50}s of 1.6 μM and 0.99 μM in Ca and GIRK, respectively) and the best efficacy (116% and 72% for Ca and GIRK activity, respectively) in both rat cell lines. Furthermore, **21a** displayed ~1% free fraction (f_u = 0.01) in both rat and mouse, modest rat predicted hepatic clearance (CL_{HEP} = 46.9 mL/min/kg) and favorable CNS exposure in rat (K_p = 4.78, $K_{p,uu}$ = 0.96) and mouse (K_p = 2.74, $K_{p,uu}$ = 0.23). In a discrete IV/PO PK study, **21a** displayed a 7.5 hour half-life and good oral bioavailability (69.5% F).[39]

Table 3. *In vitro* Pharmacology, DMPK and plasma:brain level (PBL) data for select $mGlu_7$ PAMs **20e**, **21a**, **21c** and **23g**.

Property	**20e**	**21a**	**21c**	**23g**
MW	418	383	408	417
cLogP	3.98	4.38	5.22	3.83
TPSA	61.1	51.8	52.8	55.1
***In vitro* Pharmacology[a]**				
Rat Calcium Assay				
EC_{50} (μM)	1.6	1.6	0.83	1.3
pEC_{50}±SEM	5.81±0.1	5.80±0.1	6.08±0.11	5.89±0.13
[%L-AP_4 max±SEM]	84.8±17.1	116.6±12.3	82.0±3.6	75.7±14.1
Rat GIRK Assay				
EC_{50} (μM)	1.0	0.99	0.75	0.71
pEC_{50}±SEM	5.99±0.1	6.00±0.1	6.12±0.07	6.15±0.14
[%L-AP_4 max±SEM]	62.2±9.5	62.8±3.4	54.5±3.8	29.5±7.1
DAT (K_i/IC_{50}) μM	>10	>10	>10	>10
***In vitro* PK parameters**				
Rat CL_{HEP} (mL/min/kg)	54.0	46.9	50.7	58.6
mouse CL_{HEP} (mL/min/kg),	75.8	84.4	76.2	76.2

Rat f_u (plasma) [Rat f_u (brain)]	0.03 [0.006]	0.01 [0.002]	0.005 [0.001]	0.01 [0.002]
Mouse f_u (plasma) [Mouse f_u (brain)]	0.02 [0.01]	0.01 [0.001]	0.004 [0.001]	0.01 [0.002]
Rat PBL (IV, 0.2 mg/kg)				
K_p	4.36	4.78	4.99	6.84
$K_{p,uu}$	0.79	0.96	1.00	1.24
Mouse PBL (IP, 10 mg/kg)				
K_p	ND	2.74	ND	ND
$K_{p,uu}$	ND	0.23	ND	ND

[a]ND = not determined.

Figure 7A highlights the $mGlu_7$ PAM activity of **21a** in our rat Ca and GIRK lines, as well as human $mGlu_7$, where **21a** displays comparable potency and efficacy and no agonist activity; thus a pure $mGlu_7$ PAM. Importantly, **21a** was inactive (EC_{50} > 30 μM; >10 μM at $mGlu_8$) at the other mGlu receptors (**Figure 7B**), and thus representing the first-in-class, selective $mGlu_7$ PAM. Beyond mGlu selectivity, **21a** was evaluated in a Eurofin Lead Profiling Screen of 68 GPCRs, ion channels and transporters and found to possess no ancillary pharmacology (no inhibition >50%@10 μM) except for at sigma 1 (77%@10 μM, binding IC_{50} = 3.5 μM).

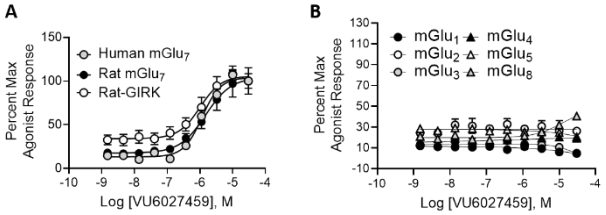

Figure 7. Molecular pharmacology profile of $mGlu_7$ PAM **21a** (VU6027459). A) $mGlu_7$ PAM concentration-response curves on human $mGlu_7$, rat $mGlu_7$ (calcium) and rat $mGlu_7$ (GIRK). B) PAM concentration response curves for **21a** on $mGlu_{1,2,3,4,5,8}$ showing no activity up to 30 μM; the exception was week PAM activity at $mGlu_8$ above 10 μM.

In summary, by virtue of the first described 'molecular switch' within a series of $mGlu_7$ NAMs, the first-in-class $mGlu_7$ PAMs were identified. Steep SAR in the optimization campaign eventually led to the discovery of **21a** (VU06027459), a highly selective and CNS penetrant tool compound, suitable for exploring the role of selective $mGlu_7$ activation *in vitro* and *in vivo*. Results from ongoing *in vivo* work in Rett models and other rodent disease models will be reported in due course.

AUTHOR INFORMATION

Corresponding Authors

*(CWL). Phone: 1 615-322-8700. Fax: 1 615-936-4381. Email: craig.lindsley@vanderbilt.edu. *(CMN). Phone: 1-615-343-4303. E-mail: colllen.niswender@vanderbilt.edu

Author Contributions

CWL and CMN drafted/corrected the manuscript and directed the science. CWR, JJK, MJW, JPW performed the chemical synthesis. CWL and CMN oversaw the target selection and interpreted the biological data. AH, YM, ALR and PJC performed the *in vitro* molecular pharmacology studies. ALB performed the *in vitro* and *in vivo* DMPK studies. All authors have given approval to the final version of the manuscript.

Acknowledgement

The authors would also like to thank the NIH (NIMH, R01MH113543 to CMN and CWL), R01MH104158 (to CMN), William K. Warren, Jr. and the William K. Warren Foundation who funded the William K. Warren, Jr. Chair in Medicine (to C.W.L.) and endowed the Warren Center for Neuroscience Drug Discovery.

ASSOCIATED CONTENT

Supporting Information. General methods for the synthesis and characterization of all compounds, and methods for the *in vitro* and *in vivo* DMPK protocols and supplemental figures. This material is available free of charge via the Internet at http://pubs.acs.org.

ABBREVIATIONS

PAM, positive allosteric modulator; PBL, plasma:brain level; DMPK, drug metabolism and pharmacokinetics; DAT, dopamine transporter

REFERENCES

(1) Niswender, C. M.; Conn, P. J. Metabotropic glutamate receptors: physiology, pharmacology, and disease. *Annu. Rev. Pharmacol. Toxicol.* **2010**, *50*, 295−322.
(2) Lindsley, C. W.; Emmitte, K. A.; Hopkins, C. R.; Bridges, T. M.; Gregory, K. A.; Niswender, C. M.; Conn, P. J. Practical strategies and concepts in GPCR allosteric modulator discovery: Recent advances with metabotropic glutamate receptors. *Chem. Rev.* **2016**, *116*, 6707− 6741.
(3) Mitsukawa, K.; Yamamoto, R.; Ofner, S.; Nozulak, J.; Pescott, O.; Lukic, S.; Stoehr, N.; Mombereau, C.; Kuhn, R.; McAllister, K. H.; van der Putten, H.; Cryan, J. F.; Flor, P. J. A selective metabotropic glutamate receptor 7 agonist: Activation of receptor signaling via an allosteric site modulates stress parameters *in vivo*. *Proc. Natl. Acad. Sci.* **2005**, *102*, 18712-18717.
(4) Sukoff Rizzo, S. J.; Leonard, S. K.; Gilbert, A.; Dollings, P.; Smith, D. L.; Zhang, M-Y.; Di, L.; Platt, B. J.; Neal, S.; Dwyer, J. M.; Bender, C. N.; Zhang, J.; Lock, T.; Kowal, D.; Kramer, A.; Randall, A.; Huselton, C.; Vishwanathan, K.; Tse, S. Y.; Butera, J.; Ring, R. H.; Rosenweig-Lipson, S.; Hughes, Z. A.; Dunlop, J. The metabotropic glutamate receptor 7 allosteric modulator AMN082: a monoaminergic agent in disguise? *J. Pharmacol. Exp. Ther.* **2011**, *338*, 345-352.
(5) Kalinichev, M.; Rouillier, M.; Girard, F.; Royer-Urios, I.; Bournique, B.; Finn, T.; Charvin, D.; Campo, B.; Le Poul, E.; Mutel, V.; Poli, S.; Neale, S. A.; Salt, T. E.; Lutjens, R. ADX71743, a potent and selective negative allosteric modulator of metabotropic glutamate receptor 7: in vitro and in vivo characterization. *J. Pharmacol. Exp. Ther.* **2013**, *3*, 624−636.
(6) Tassin, V.; Girard, B.; Chotte, A.; Fontanaud, P.; Rigault, D.; Kalinichev, M.; Perroy, J.; Acher, F.; Fagni, L.; Bertaso, F. Phasic and tonic mGlu7 receptor activity modulates the thalamocortical network. *Front. Neural Circuits* **2016**, *10:31*. doi: 10.3389/fncir.2016.00031.
(7) Sansig, G.; Bushell, T. J.; Clarke, V. R.; Rozov, A.; Burnashev, N.; Portet, C.; Gasparini, F.; Schmutz, M.; Klebs, K.; Shigemoto, R.; Flor, P. J.; Kuhn, R.; Knoepfel, T.; Schroeder, M.; Hampson, D. R.; Collett, V. J.; Zhang, C.; Duvoisin, R. M.; Collingridge, G. L.; van Der Putten, H. Increased seizure susceptibility in mice lacking metabotropic glutamate receptor 7. *J. Neurosci.* **2001**, *21*, 8734−8745.
(8) Goddyn, H.; Callaerts-Vegh, Z.; Stroobants, S.; Dirikx, T.; Vansteenwegen, D.; Hermans, D.; van der Putten, H.; D'Hooge, R. Deficits

in acquisition and extinction of conditioned responses in mGluR7 knockout mice. *Neurobiol. Learn. Mem.* **2008**, *90*, 103−111.
(9) Palucha, A.; Klak, K.; Branski, P.; van der Putten, H.; Flor, P. J.; Pilc, A. Activation of the mGlu7 receptor elicits antidepressant-like effects in mice. *Psychopharmacology* **2007**, *194*, 555−562.
(10) Callaerts-Vegh, Z.; Beckers, T.; Ball, S. M.; Baeyens, F.; Callaerts, P. F.; Cryan, J. F.; Molnar, E.; D'Hooge, R. Concomitant deficits in working memory and fear extinction are functionally dissociated from reduced anxiety in metabotropic glutamate receptor 7-deficient mice. *J. Neurosci.* **2006**, *26*, 6573−6582.
(11) Mitsukawa, K.; Mombereau, C.; Lotscher, E.; Uzunov, D. P.; van der Putten, H.; Flor, P. J.; Cryan, J. F. Metabotropic Glutamate Receptor Subtype 7 Ablation Causes Dysregulation of the HPA Axis and Increases Hippocampal BDNF Protein Levels: Implications for Stress-Related Psychiatric Disorders. *Neuropsychopharmacology* **2006**, *31*, 1112−1122.
(12) Holscher, C.; Schmid, S.; Pilz, P. K.; Sansig, G.; van der Putten, H.; Plappert, C. F. Lack of the metabotropic glutamate receptor subtype 7 selectively modulates Theta rhythm and working memory. *Learn. Mem.* **2005**, *12*, 450−455.
(13) Holscher, C.; Schmid, S.; Pilz, P. K.; Sansig, G.; van der Putten, H.; Plappert, C. F. Lack of the metabotropic glutamate receptor subtype 7 selectively impairs short-term working memory but not long-term memory. *Behav. Brain Res.* **2004**, *154*, 473−481.
(14) Bushell, T. J.; Sansig, G.; Collett, V. J.; van der Putten, H.; Collingridge, G. L. Altered short-term synaptic plasticity in mice lacking the metabotropic glutamate receptor mGlu7. *Sci. World J.* **2002**, *2*, 730−737.
(15) Masugi, M.; Yokoi, M.; Shigemoto, R.; Muguruma, K.; Watanabe, Y.; Sansig, G.; van der Putten, H.; Nakanishi, S. Metabotropic glutamate receptor subtype 7 ablation causes deficit in fear response and conditioned taste aversion. *J. Neurosci.* **1999**, *19*, 955−963.
(16) Breen, G.; Webb, B. T.; Butler, A. W.; van den Oord, E. J.; Tozzi, F.; Craddock, N.; Gill, M.; Korszun, A.; Maier, W.; Middleton, L.; Mors, O.; Owen, M. J.; Cohen-Woods, S.; Perry, J.; Galwey, N. W.; Upmanyu, R.; Craig, I.; Lewis, C. M.; Ng, M.; Brewster, S.; Preisig, M.; Rietschel, M.; Jones, L.; Knight, J.; Rice, J.; Muglia, P.; Farmer, A. E.; McGuffin, P. A genome-wide significant linkage for severe depression on chromosome 3: the depression network study. *Am. J. Psychiatry* **2011**, *168*, 840−847.
(17) Ganda, C.; Schwab, S. G.; Amir, N.; Heriani, H.; Irmansyah, I.; Kusumawardhani, A.; Nasrun, M.; Widyawati, I.; Maier, W.; Wildenauer, D. B. A family-based association study of DNA sequence variants in GRM7 with schizophrenia in an Indonesian population. *Int. J. Neuropsychopharmacol.* **2009**, *12*, 1283−1289.
(18) Mick, E.; Neale, B.; Middleton, F. A.; McGough, J. J.; Faraone, S. V. Genome-wide association study of response to methylphenidate in 187 children with attention-deficit/hyperactivity disorder. *Am. J. Med. Genet., Part B* **2008**, *147B*, 1412−1418.
(19) Yang, Y.; Pan, C. Role of metabotropic glutamate receptor 7 in autism spectrum disorders: a pilot study. *Life Sci.* **2013**, *92*, 149−153.
(20) Elia, J.; Glessner, J. T.; et al. Genome-wide copy number variation study associated metabotropic glutamate receptor gene networks with attention deficit hyperactivity disorder. *Nat. Genet.* **2012**, *44*, 78−84.
(21) Douglas, L. N.; McGuire, A. B.; Manzardo, A. M.; Butler, M. G. High-resolution chromosome ideogram representation of recognized genes for bipolar disorder. *Gene* **2016**, *586*, 136−147.
(22) Shyn, S. I.; Shi, J.; Kraft, J. B.; Potash, J. B.; Knowles, J. A.; Weissman, M. M.; Garriock, H. A.; Yokoyama, J. S.; McGrath, P. J.; Peters, E. J.; Scheftner, W. A.; Coryell, W.; Lawson, W. B.; Jancic, D.; Gejman, P. V.; Sanders, A. R.; Holmans, P.; Slager, S. L.; Levinson, D. F.; Hamilton, S. P. Novel loci for major depression identified by genome-wide association study of Sequenced Treatment Alternatives to Relieve Depression and meta-analysis of three studies. *Mol. Psychiatry* **2011**, *16*, 202−215.
(23) Li, W.; Ju, K.; Li, Z.; He, K.; Chen, J.; Wang, Q.; Yang, B.; An, L.; Feng, G.; Sun, W.; Zhou, J.; Zhang, S.; Song, P.; Khan, R.; Ji, W.; Shi, Y. Significant association of GRM7 and GRM8 genes with schizophrenia and major depressive disorder in the Han Chinese population. *Eur. Neuropsychopharmacol.* **2016**, *26*, 136−146.
(24) Park, S.; Kim, B. N.; Cho, S. C.; Kim, J. W.; Kim, J. I.; Shin, M. S.; Yoo, H. J.; Han, D. H.; Cheong, J. H. The metabotropic glutamate receptor subtype 7 rs3792452 polymorphism is associated with the response to methylphenidate in children with attention-deficit/ hyperactivity disorder. *J. Child Adolesc. Psychopharmacol.* **2014**, *24*, 223−227.
(25) Park, S.; Jung, S. W.; Kim, B. N.; Cho, S. C.; Shin, M. S.; Kim, J. W.; Yoo, H. J.; Cho, D. Y.; Chung, U. S.; Son, J. W.; Kim, H. W. Association between GRM7 rs3792452 polymorphism and attention-deficit/hyperactivity disorder in a Korean sample. *Behav. Brain Funct.* **2013**, *9*,1−11.
(26) Kandaswamy, R.; McQuillin, A.; Curtis, D.; Gurling, H. Allelic association, DNA resequencing and copy number variation at the metabotropic glutamate receptor GRM7 gene locus in bipolar disorder. *Am. J. Med. Genet., Part B* **2014**, *165B*, 365−372.
(27) Liu, Y.; Zhang, Y.; Zhao, D.; Dong, R.; Yang, X.; Tammimies, K.; Uddin, M.; Scherer, S. W.; Gai, Z. Rare de novo deletion of metabotropic glutamate receptor 7 (GRM7) gene in a patient with autism spectrum disorder. *Am. J. Med. Genet., Part B* **2015**, *168B*, 258− 264.
(28) Charng, W. L.; Karaca, E.; Coban-Akdemir, Z.; Gambin, T.; Atik, M. M.; Gu, S.; Posey, J. E.; Jhangiani, J. A.; Muzny, D. M.; Doddapaneni, H.; Hu, J.; Boerwinkle, E.; Gibbs, R. A.; Rosenfeld, J. A.; Cui, H.; Xia, F.; Manickam, K.; Yang, Y.; Faqeih, E. A.; Al Asmari, A.; Saleh, M. A.; El-Hattab, A. W.; Lupski, J. R. Exome sequencing in mostly consanguineous Arab families with neurological disease provides a high potential molecular diagnosis rate. *BMC Med. Genomics* **2016**, *19*, 42−54.
(29) Reuter, M. S.; Tawamie, H.; et al. Diagnostic yield and novel candidate genes by exome sequencing in 152 consanguineous families with neurodevelopmental disorders. *JAMA Psychiatry* **2017**, *74*, 293− 299.
(30) Fisher, N. M.; Seto, M.; Lindsley, C. W.; Niswender, C. M. Metabotropic Glutamate Receptor 7: A new therapeutic target in neurodevelopmental disorders. *Front. Mol. Neurosci.* **2018**, *11*, 387.
(31) Kalinichev, M.; Le Poul, E.; Boléa, C.; Girard, F.; Campo, B.; Fonsi, M.; Royer-Urios, I.; Browne, S. E.; Uslaner, J. M.; Davis, M. J.; Raber, J.; Duvoisin, R.; Bate, S. T.; Reynolds, I. J.; Poli, S.; Celanire, S. Characterization of the novel positive allosteric modulator of the metabotropic glutamate receptor 4 ADX88178 in rodent models of neuropsychiatric disorders. *J. Pharmacol. Exp. Ther.* **2014**, *350*, 495-505.
(32) Jalan-Sakrikar, N.; Field, J. R.; Klar, R.; Mattmann, M. E.; Gregory, K. J.; Zamorano, R.; Engers, D. W.; Bollinger, S. R.; Weaver, C. D.; Days, E.; Lewis, L. M.; Utley, T. J.; Hurtado, M.; Rigault, D.; Acher, F.; Walker, A. G.; Melancon, B. J.; Wood, M. R.; Lindsley, C. W.; Conn, P. J.; Xiang, Z.; Hopkins, C. R.; Niswender, C. M. Identification of positive allosteric modulators VU0155094 (ML397) and VU0422288 (ML396) reveals new insights into the biology of metabotropic glutamate receptor 7. *ACS Chem. Neurosci.* **2014**, *5*, 1221−1237.
(33) Abe, M.; Seto, M.; Gogliotti, R. G.; Loch, M. T.; Bollinger, K. A.; Chang, S.; Engelberg, E. M.; Luscombe, V. B.; Harp, J. M.; Bubser, M.; Engers, D. W.; Jones, C. K.; Rodriguez, A. L.; Blobaum, A. L.; Conn, P. J.; Niswender, C. M.; Lindsley, C. W. Discovery of VU6005649, a CNS penetrant mGlu7/8 receptor PAM from a series of pyrazolo[1,5-a]pyrimidines. *ACS Med. Chem. Lett.* **2017**, *8*, 1110− 1115.
(34) Reed, C. W.; Yohn, S. E.; Washecheck, J. P.; Roenfanz, H. F.; Quitalig, M. C.; Luscombe, V. B.; Jenkins, M. T.; Rodriguez, A. L.; Engers, D. W.; Blobaum, A. L.; Conn, P. J.; Niswender, C. M.; Lindsley, C. W. Discovery of an orally bioavailable and central nervous system (CNS) penetrant $mGlu_7$ negative allosteric modulator (NAM) *in vivo* tool compound: *N*-(2-(1*H*-1,2,4-triazol-1-yl)-5-(trifluoromethoxy)phenyl)-4-(cyclopropylmethoxy)-3-methoxybenzamide (VU6012962). *J. Med. Chem.* **2019**, *62*, 1690-1695.
(35) Gogliotti, R. G.; Senter, R. K.; Fisher, N. M.; Adams, J.; Zamorano, R.; Walker, A. G.; Blobaum, A. L.; Engers, D. W.; Hopkins, C. R.; Daniels, J. S.; Jones, C. K.; Lindsley, C. W.; Xiang, Z.; Conn, P. J.; Niswender, C. M. Metabotropic Glutamate Receptor 7 Allosteric Modulation Rescues Long Term Potentiation, Cognition and Apneas in Mecp2-Deficient Mice. *Sci. Transl. Med.* **2017**, *9*, eaai7459.
(36) Reed, C. W.; McGowan, K. M.; Spearing, P. K.; Stansley, B. J.; Roenfanz, H. F.; Engers, D. W.; Rodriguez, A. L.; Engelberg, E. M.; Luscombe, V. B.; Loch, M. T.; Remke, D. H.; Rook, J. M.; Blobaum, A. L.; Conn, P. J.; Niswender, C. M.; Lindsley, C. W. VU6010608, a novel mGlu7 NAM from a series of N-(2-(1H-1,2,4-triazol-1-yl)-5(trifluoromethoxy)phenyl)benzamides. *ACS Med. Chem. Lett.* **2017**, *8*, 1326−1330.
(37) Reed, C. W.; Washecheck, J. P.; Quitalig, M. C.; Jenkins, M. T.; Rodriguez, A. L.; Engers, D. W.; Blobaum, A. L.; Conn, P. J.; Niswender, C. M.; Lindsley, C. W. Surveying heterocycles as amide bioisosteres within a series of $mGlu_7$ NAMs: discovery of VU6019278. *Bioorg. Med. Chem. Lett.* **2019**, *29*, 1211-1214.

(38) Kalbfleisch, J. J.; Reed, C. W.; Park, C.; Spearing, P. K.; Quitalig, M. C.; Jenkins, M. T.; Rodriguez, A. L.; Blobaum, A. L.; Conn, P. J.; Niswender, C. M.; Lindsley, C. W. Synthesis and SAR of a series of $mGlu_7$ NAMs based on an ethyl-8-methoxy-4-(4-phenylpiperazin-1-yl)quinoline carboxylate core. *Bioorg. Med. Chem. Lett.* Manuscript submitted.
(39) See Supporting Information

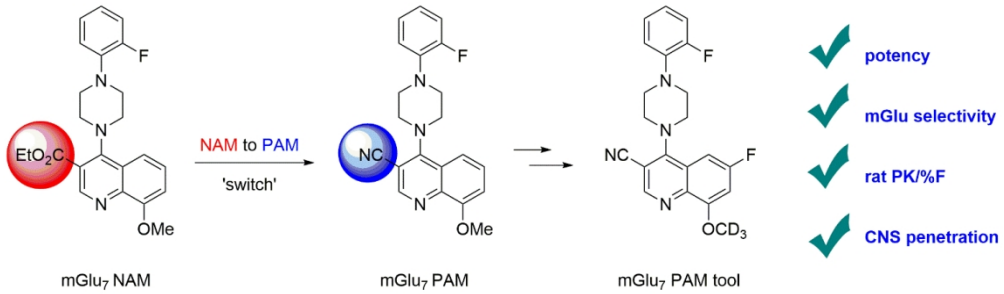

177x52mm (220 x 220 DPI)

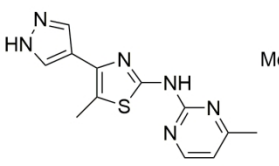

1, ADX88178
$mGlu_4$ EC_{50} = 52 nM
$mGlu_7$ EC_{50} >10 μM
$mGlu_8$ EC_{50} = 1.2 μM

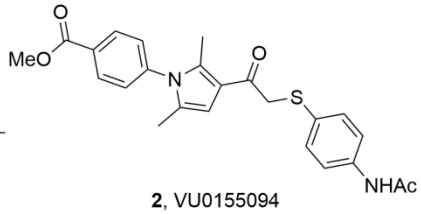

2, VU0155094
$mGlu_4$ EC_{50} = 3.2 μM
$mGlu_7$ EC_{50} = 1.5 μM
$mGlu_8$ EC_{50} = 900 nM

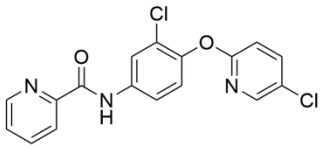

3, VU0422288
$mGlu_4$ EC_{50} = 108 nM
$mGlu_7$ EC_{50} = 146 nM
$mGlu_8$ EC_{50} = 125 nM

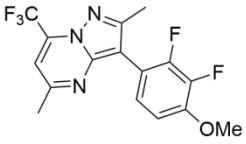

4, VU6005649
$mGlu_4$ EC_{50} >10 μM
$mGlu_7$ EC_{50} = 649 nM
$mGlu_8$ EC_{50} = 2.6 μM

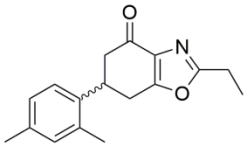

5, ADX71743
$mGlu_7$ EC_{50} = 650 nM
other mGlus > 10 μM

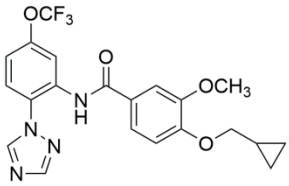

6, VU6012962
$mGlu_7$ EC_{50} = 347 nM
other mGlus > 10 μM

175x110mm (300 x 300 DPI)

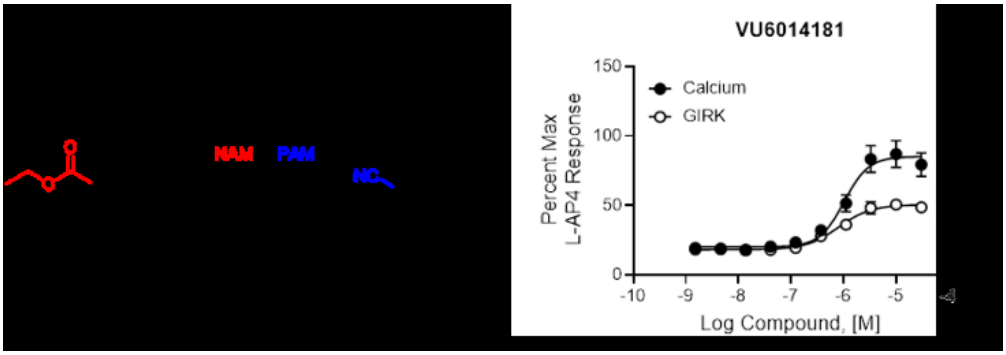

84x29mm (220 x 220 DPI)

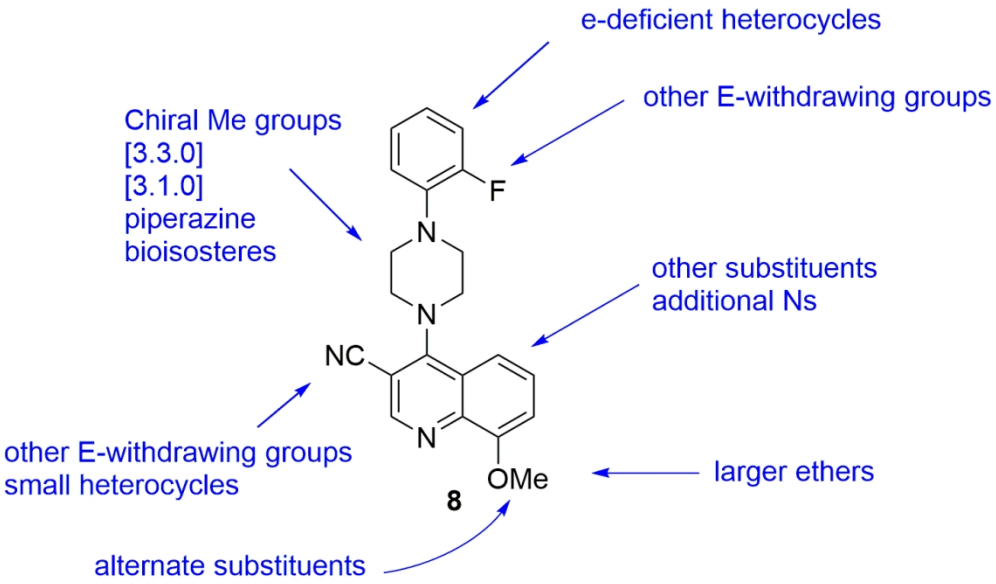

123x72mm (300 x 300 DPI)

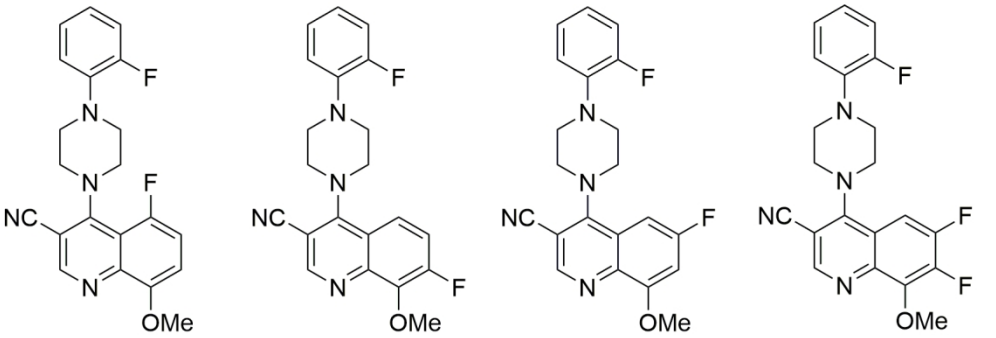

14a
EC_{50} > 10 μM
35% L-AP_4 Max
DAT IC_{50} = 4 μM

14b
EC_{50} = 1.8 μM
53% L-AP_4 Max
DAT IC_{50} = 3 μM

14c
EC_{50} = 1.4 μM
98% L-AP_4 Max
DAT IC_{50} > 10 μM

14d
EC_{50} = 1.1 μM
62% L-AP_4 Max
DAT IC_{50} > 10 μM

145x72mm (300 x 300 DPI)

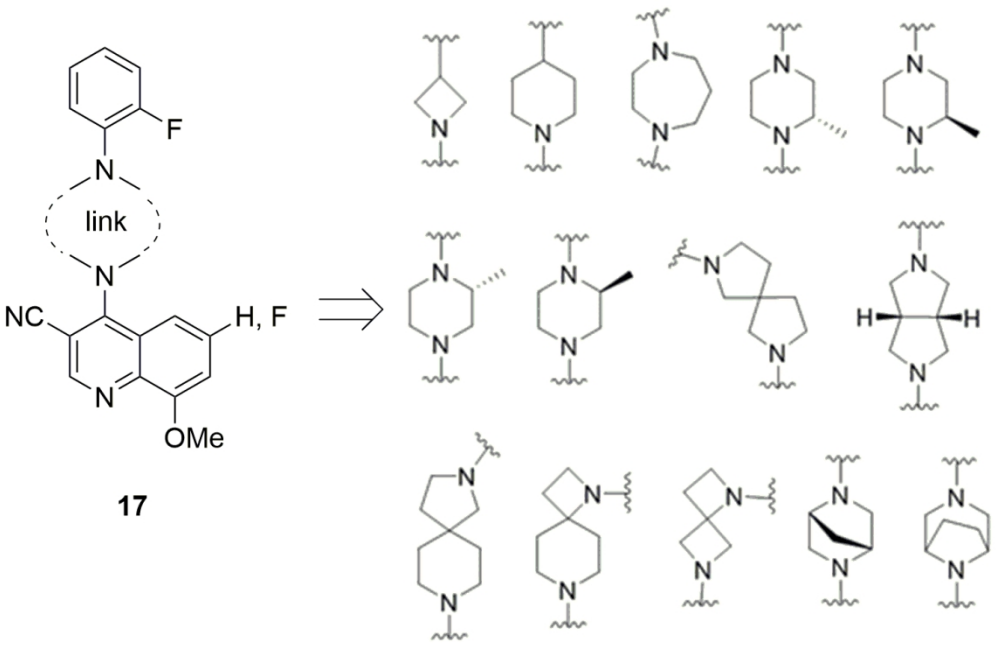

125x81mm (300 x 300 DPI)

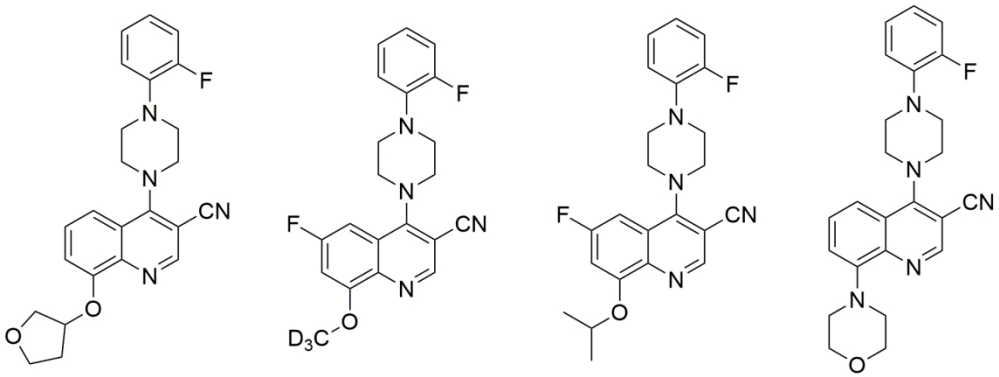

20e
VU6027271

21a
VU6027459

21c
VU6027446

23g
VU6027452

155x73mm (300 x 300 DPI)

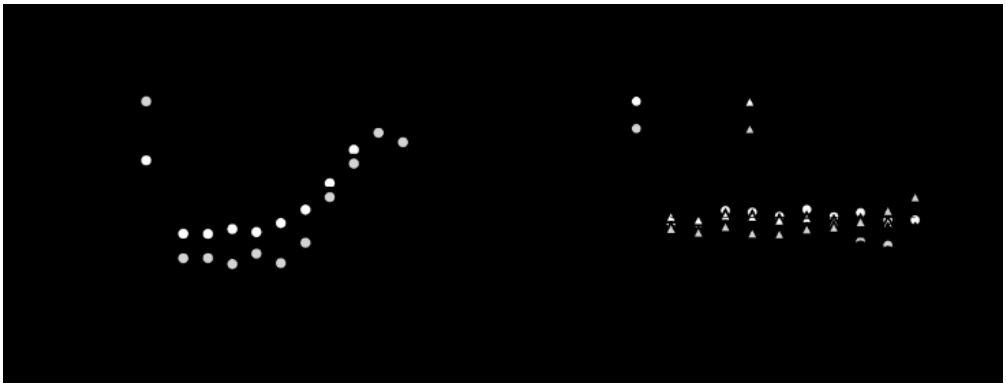

84x32mm (220 x 220 DPI)

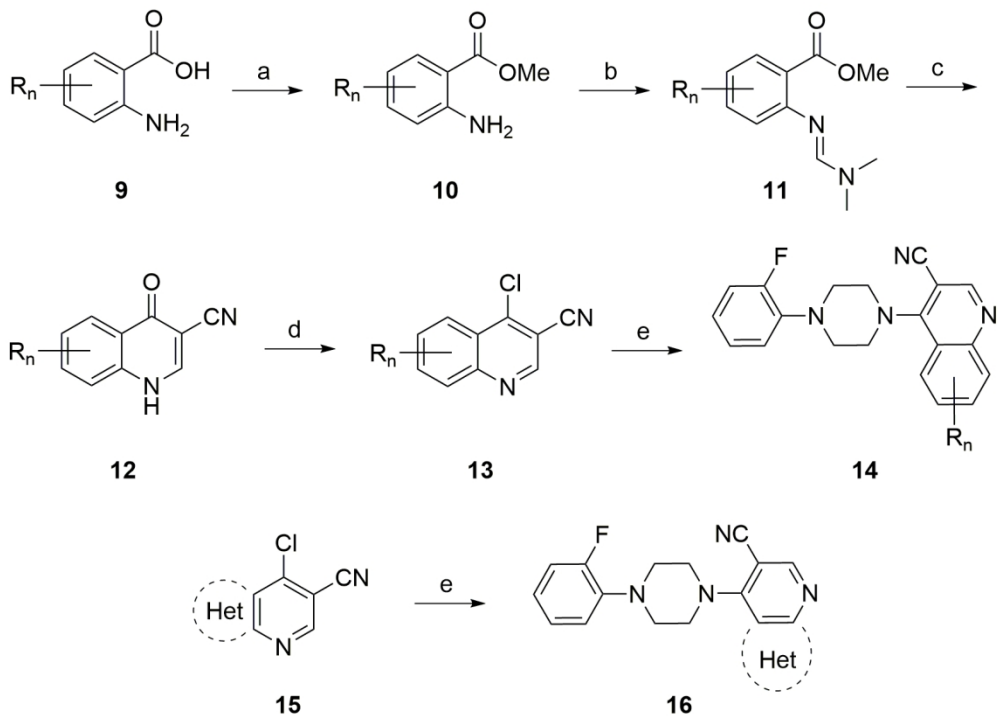

146x105mm (300 x 300 DPI)

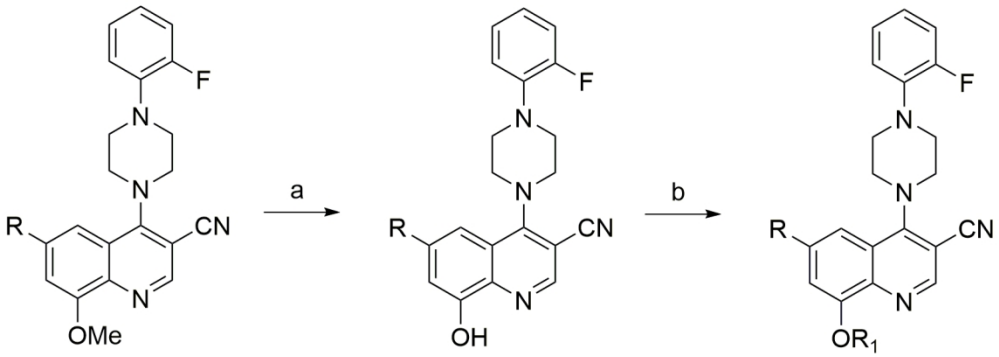

8, R = H
14c, R = F

18, R = H
19, R = F

20, R = H
21, R = F

139x62mm (300 x 300 DPI)

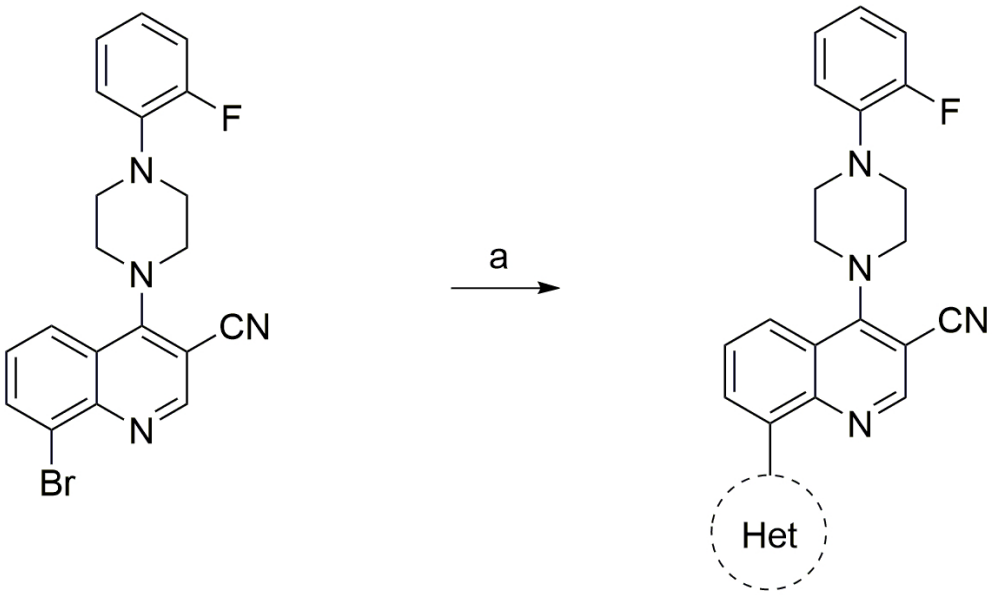

22 **23**

97x64mm (300 x 300 DPI)